Kinetics of high pressure leaching of nickel lateritic ore "Silcrete"

[1]Stopić, S., Friedrich, B., Fuchs, R.
IME Process Metallurgy and Metal Recycling
Intzestrasse 3
Aachen, Germany D-52072

Anastasijević, N.
Outokumpu Technology GmbH, Metals Processing
Ludwig-Erhard Strasse 21
Oberursel, Germany, D-61440

Abstract

This study presents the results obtained from a thermodynamic and kinetics study of nickel lateritic ore leaching in sulphuric acid solutions at high pressure conditions. Evaluation of thermodynamic equilibrium in system Me-S-H_2O is considered by Eh-pH diagrams in Software "Factsage". Domains of stability and co-existing scope of different form and compound are present for Ni, Co, Mg, Al and Fe at 250°C. Nickel lateritic ore "Silcrete", Western Australia was used for the leaching experiments in a titanium autoclave equipped with acid injection system and a sampling unit at high pressure of 40 bar. The conditions examined were at temperature of 250°C, acid- to - ore ratio a/o between 0.4 and 0.5 with solid percent of 10 % and stirring speed 1500 rpm. Under these conditions the maximal value of 69 % nickel, 73 % of magnesium and of 81 % cobalt extraction was attained in 15 min. The increase of acid to ore ratio from 0.4 to 0.5 increases nickel and cobalt dissolution, and the leach selectivity was increased three times.

1. INTRODUCTION

Pressure acid leaching PAL is the current process of choice for greenfields nickel laterite projects [1-3]. The extension of the process from tropical limonites to Western Australian laterites is a new approach, and as such the behavior of the differing

---

[1] E-Mail: sstopic@ime-aachen.de; Fax: + 49 (0) 241 80 92 154

minerals in tropical and arid laterites during leaching is widely examined. The fundamentals of PAL of iron oxides were examined by Tindall and Muir [4], using synthetic goethite as a model ore. It was found that goethite transforms to hematite by a dissolution and re-precipitation mechanism. The leaching rate was depend on the acid concentration, the slurry oxidation potential, and the type of cations in the solution. It is also confirmed that nontronite reacted more readily than iron oxides.

Rubisov and Papangelakis [5] have developed a comprehensive model estimating and including the kinetics of Co, Fe, Al, Mn and Ni dissolution in the temperature range from 230°C to 270°C. The resulting model is capable of predicting the Ni extraction and the concentration of major impurities during autoclave operation for a wide variety of process conditions and feed compositions. It was implemented in a simulation.

The future trend for nickel production is expected to involve the processing of laterites, which account for about 70 % of the world's resources, by means of efficient PAL and SX-EW facilities [6-8].

The aim of this paper is to investigate the behavior for nickel laterite from deposits in Silcrete, Western Australia with the use of sulfuric acid in an autoclave at temperature at 250°C, which is one of the optimal parameter for this leach process. During a thermodynamic and kinetics analysis should be investigated a selectivity of the leaching process.

2. THERMODYNAMICAL ANALYSIS

The dominant leaching oxidation reactions with sulphuric acid can be further identified from the corresponding E-pH diagrams (Fig. 1.a-1.e). Especially the dissolution of Ni, Co and Mg from nickel lateritic ore is desirable.

Fig. 1.a. E-pH diagram of an nickel/acid leaching system with the molar ratio 0.67>(S/S+Ni)<1 at 250°C

In sulphuric acid medium with the molar ratio 0.67>(S/S+Ni)<1 at 250°C the area of ions Ni^{2+} are typical when the values of oxidizing potential amount E= 0.25 and 1.0 V with pH values between 0 and 0.25. Nickel sulphide is stable in medium in wide range of pH.

For diagram Co-S-H-O (Fig. 1.b) more wide domain of existence is typical for ions of Co^{2+} up to pH= 1. In the presence of sulphur the sulphide area appears. Elemental cobalt has a large domain of existence in water solution, but in the presence of sulphur this domain essentially decreases. Some sizes of areas belong to cobalt oxide compounds, especially when pH>1, although oxides and hydroxides of nickel and cobalt are not stable in the acid area. In case of Co_3S_4 presence, its oxidizing misses the stage of monosulphide generation.

In acid medium big areas of ions Mg^{2+} are typical (Fig. 1.c)

Fig. 1.b. E-pH diagram of an cobalt/acid leaching system with the molar ratio 0.67>(S/S+Co)<1 at 250°C

Fig. 1.c. E-pH diagram of an magnesium/acid leaching system with the molar ratio 0.67>(S/S+Mg)<1 at 250°C

Fig. 1.d. shows the zone of stability for FeS, FeS_2 and Fe. The domains occupied by iron oxides, especially Fe_2O_3, are very representative. The area of ions Fe^{2+} are typical when the values of oxidizing potential amount E= -0.4 and 0 V with pH values

below 0.6. For FeS_2 the probability of elemental sulphur generation exists ion only when pH<0 and moderate temperature. With a high value of pH a generation of ion SO_4^{2-} is probable.

Fig. 1.d. E-pH diagram of an iron/acid leaching system with the molar ratio 0.67>(S/S+Fe)<1 at 250°C

Fig. 1.e. shows the zone of stability for aluminium compounds. Hydrogen sulphide is typical for areas with low oxidizing potential. The area of ions Al^{3+} are not present.

Fig. 1.e. E-pH diagram of an aluminium/acid leaching system with the molar ratio 0.67>(S/S+Al)<1 at 250°C

3. EXPERIMENTAL

3.1. Material

The ore composition used in this experiment can be seen from the Table 1.

Table 1: Ore sample composition

The particle size distribution are showed on Figure 2.

Figure 2: Particle size distribution in Silcrete ore after a sieving

The measured density of laterite suspension by "Helos Sympatec" Software amounts 2.71 g/cm^3.

3.2. Equipment

Under high pressure leaching conditions tests were performed in a 2 dm^3 autoclave, manufactured by the Autoclave Engineers, USA, which is part of a 3 reactor system from 1- 50 dm^3 at IME, RWTH University, Aachen. The working procedure is described in detail in Reference [9, 10]. After the end of experiments, solutions aliquots were filtered und analysed in order to determine Ni, Co, Mg, Al, and Fe by ICP spectrophotometry.

The experiments were done at 250°C in time up to 15 min with 10 % solid and one higher stirring speed of 1500 rpm. Corresponding to 250°C the equilibrium vapour pressure amounted 40 bar. The acid- to- ore ratio a/o was amounted between 0.40 and 0.50 g H_2SO_4 per g ore.

3.3. Results and Discussion

15 min leaching tests was performed for "Silcrete" ore, Australia at 10 % solid in acid to ore range 0.4 and 0.5 with a stirring speed of 1500 rpm (Figure 3). The influence of stirring speed is previous explained [11]. 57 % Ni and 68 % Co extraction is attained in 15 min at 250°C, 10 % solids and 0.40 a/o ratio (Fig. 6). The change from 0.40 to 0.50 a/o ratio increased extraction of nickel up to 68 % and Co to 81 % under same conditions.

Fig. 3. Metal dissolution kinetics from "Silcrete" (10% solid, a/o=0.4, v= 1500 rpm)

Fig. 4. Metal dissolution kinetics from "Silcrete" (10% solid, a/o=0.5, v= 1500 rpm)

The increase of a/o ratio from 0.4 to 0.5 increases nickel and cobalt extraction at 250°C (Fig.4). This change of a/o ratio increases the leach selectivity (%Ni + % Co)/((%Fe + % Al) almost three times (Fig. 5). It was difficult to measure the rates of iron dissolution and precipitation separately because of the simultaneous occurrence of two reaction. Iron precipitation kinetics was recovered by subtracting the measured concentration of Fe in solution from the theoretical amount of Fe dissolved. As mentioned by Rubisov and Papangelakis [6] an iron precipitation as hematite has proceeded through the formation of basic ferric sulphate. The latter quickly converts to hematite. At higher acidities (0.5 and 0.75 mol/L) more than 90 % of Al dissolves fast within 2.5 min, making it is impossible to establish the dissolution kinetics. After this Al dissolution follows his precipitation of to the alunite .

Fig. 5. Leaching selectivity (10% solid, T=250°C, t=15 min, v= 1500 rpm)

After the leaching test and sampling at 250°C, 10 % solids, and a/o ratio of 0.4 the solids were very quickly washed, filtered and prepared for DTA and TGA analysis (Fig. 6).

Fig. 6. TGA and DTA analysis in argon for leach residue obtained by PAL of "Silcrete" under following conditions: T = 250°C; a/o = 0.4; t = 15 min;

We are assumed that high pressure leaching ore ends up the solid product that contains SiO_2, Fe_2O_3 and $(H_3O^+, Na^+)Al_3(SO_4)_2(OH)_6$. TGA showed that the mass loss obtained at 250°C amounts 7.27% at 290°C and 12.82 % at 620°C. DTA analysis shows the presence of 2 peaks (at 109.3 % and 290°C). The first peak at 109.3°C corresponds the evaporation of water. The second peak indicates the possible beginning of decomposition of alunite, formed during leaching with sulphuric acid.

4. CONCLUSION

Thermodynamic analysis shows that in sulphuric acid medium with the molar ratio 0.67>(S/S+Ni)<1 at 250°C the area of ions Ni^{2+} are typical for the values of oxidizing potential of E= 0.25 and 1.0 V with pH values between 0 and 0.25. The domains for Co^{2+} and Mg^{2+} are broader than ones of nickel and present at pH values up to 1. Domains of Fe^{3+} are present for the values of oxidizing potential between E= -0.4 and 1.0 V and with pH values up to 0.6. The presence of Al^{3+} is not found.

It was shown that Silcrete ore react readily during high pressure sulphuric acid leaching under following conditions: T= 250°C; t=15 min, v=1500 rpm: a/o = 0.4 and 0.5. Under these conditions the highest nickel extraction amounted 68 % in 15 min, but the cobalt had a higher value of 81 %. An increasing an acid to ore ratio in the autoclave increases the rate of nickel and cobalt extraction at 250°C. Leaching selectivity (%Ni + % Co)/((%Fe + % Al) increases almost three when the a/o ratio changes from 0.4 to 0.5.

5. ACKNOWLEDGMENTS

We would like to thank the Alexander von Humboldt Foundation for its research fellowships for Dr. Srećko Stopić allowing a 15 month stay at IME Process Metallurgy and Metal Recycling, RWTH Aachen, where these experiments were done.

6. REFERENCES

1. Whittington, B.I., Muir, D, 2000. Pressure acid leaching of nickel laterites: a review. Min.Pro.Ext.Met.Rev. 21, 527-600.

2. Bergman, R.A., 2003. Nickel production from low-iron laterite ores: Process description. CIM Bulletin 96 (1072), 127-138.

3. Moskalyk, R.R, A.M. Alfantazi, A.M., 2002. Nickel laterite processing and electrowinning practice. Minerals Engineering 15, 593-605.

4. Tindall, G.P, Muir, D.M., 1998. Effect of E_h on the rate and mechanism of the transformation of goethite into hematite in a high temperature acid leach process. Hydrometallurgy 47, 377-381.

5. Rubisov, D.H, Papangelakis, V.G., 2000. Sulphuric acid pressure leaching of laterites-a comprehensive model of a continuous autoclave. Hydrometallurgy 58, 89-101.

6. Georgiou, D., Papangelakis, V.G., 1998. Sulphuric acid pressure leaching of limonite laterite: chemistry and kinetics. Hydrometallurgy 49, 23-46.

7. Cheng, C.J., Urbani, M., 2003. Purification of laterite leach solutions by direct solvent extraction. Volume 3: Aqueous and Electrochemical Processing, Kongoli, F., Itagaki, K., Yamauchi, C., Sohn, H.Y. (Eds.), The Minerals, Metals, & Materials Society, San Diego, 251-265.

8. Arroyo, J.C., Gillaspie, J.D., Neudorf, D.A., Weenink., E.M., 2002. Method for leaching nickeliferous laterite. United States Patent, No. 6.379.636

9. Stopić, S., Friedrich, B,, Anastasijević, N., 2003. Kinetics of high pressure leaching of the Serbian nickel lateritic ore. Volume 1: Copper and Nickel, Dietrich, W. (Ed.), GDMB, Hanover, 189-204.

10. Havlik, T., Friedrich, B., Stopić, S., 2004. Pressure Leaching of EAF dust with sulphuric acid. Erzmetall 57 (2), 83-90.

11. Stopić, S., 2003. High pressure leaching of lateritic ore. Humboldt Kosmos 84, 34.

Tables

Table 1: Ore sample composition

Content	Si	Fe	Al	Cr	Ni	Co	Na	K	Mg	Mn
%	17.4	26.4	4.16	0.67	0.78	0.05	0.4	0.05	1.7	0.25

Figure captions:

Fig. 1.a. Eh-pH diagram of an nickel/acid leaching system with the molar ratio $0.67>(S/S+Ni)<1$ at 250°C

Fig. 1.b. Eh-pH diagram of an cobalt/acid leaching system with the molar ratio $0.67>(S/S+Co)<1$ at 250°C

Fig. 1.c. Eh-pH diagram of an magnesium/acid leaching system with the molar ratio $0.67>(S/S+Mg)<1$ at 250°C

Fig. 1.d. Eh-pH diagram of an iron/acid leaching system with the molar ratio $0.67>(S/S+Fe)<1$ at 250°C

Fig. 1.e. Eh-pH diagram of an aluminium/acid leaching system with the molar ratio $0.67>(S/S+Al)<1$ at 250°C

Figure 2. Particle size distribution in Silcrete ore after a sieving

Fig. 3. Metal dissolution kinetics from “Silcrete” (10% solid, a/o=0.4, v= 1500 rpm)

Fig. 4. Metal dissolution kinetics from “Silcrete” (10% solid, a/o=0.5, v= 1500 rpm)

Fig. 5. Leaching selectivity (10% solid, T=250°C, t=15 min, v= 1500 rpm)

Fig. 6. TGA and DTA analysis in argon for leach residue obtained by PAL of Silcrete under following conditions: T = 250°C; a/o = 0.4; t = 15 min;

Figures:

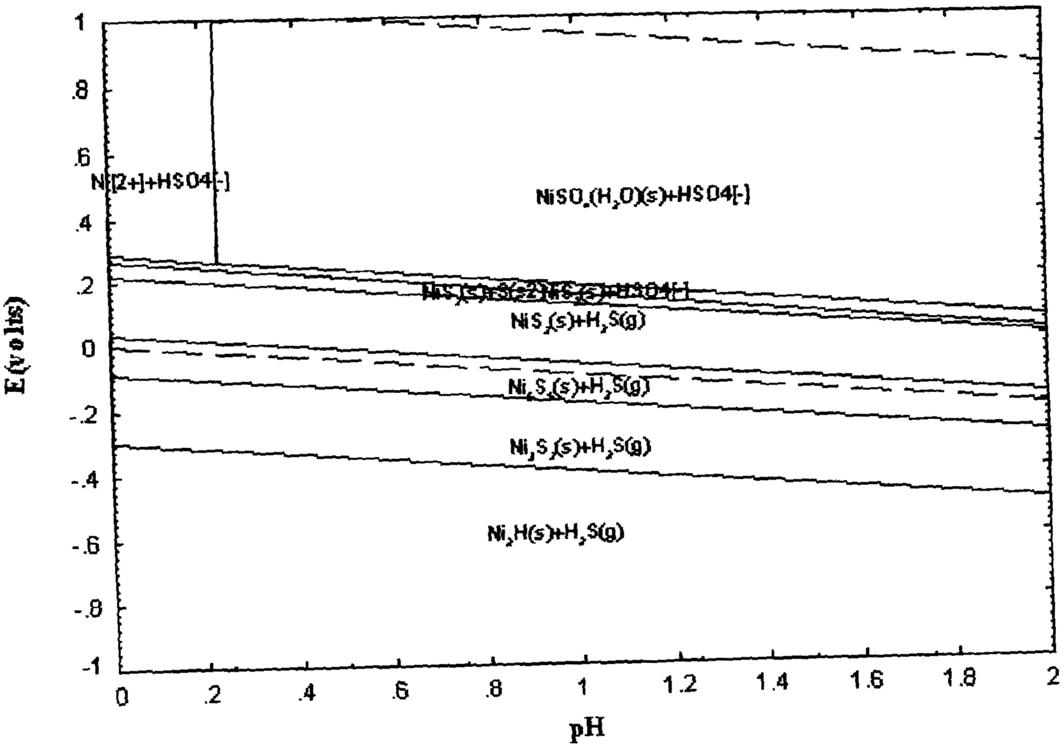

FiG. 1.a.

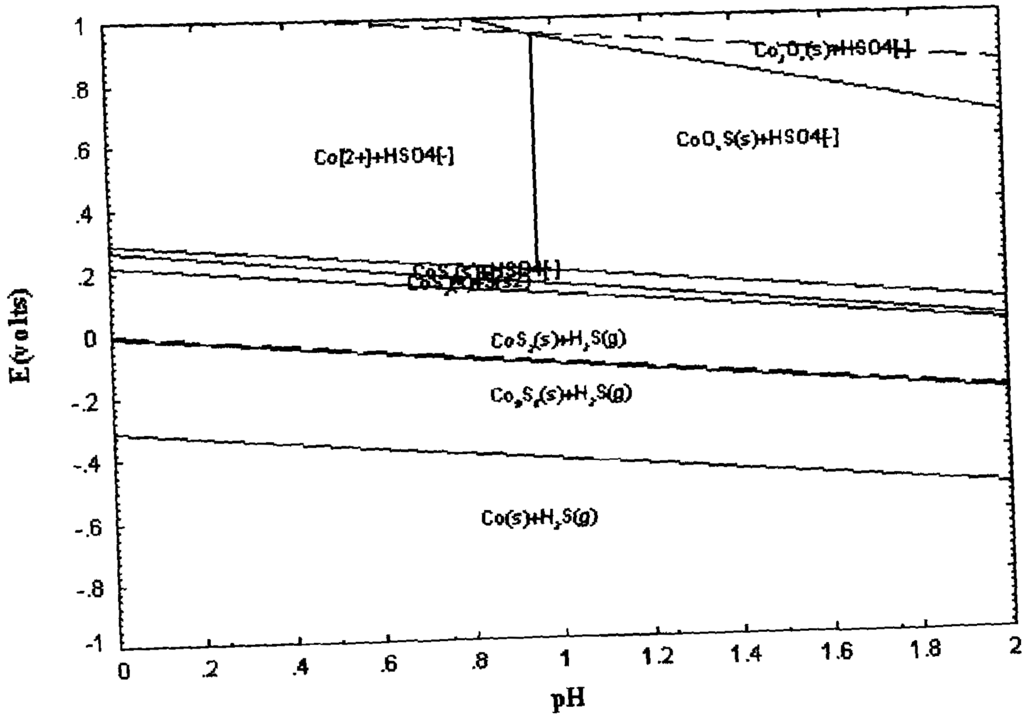

Fig. 1.b.

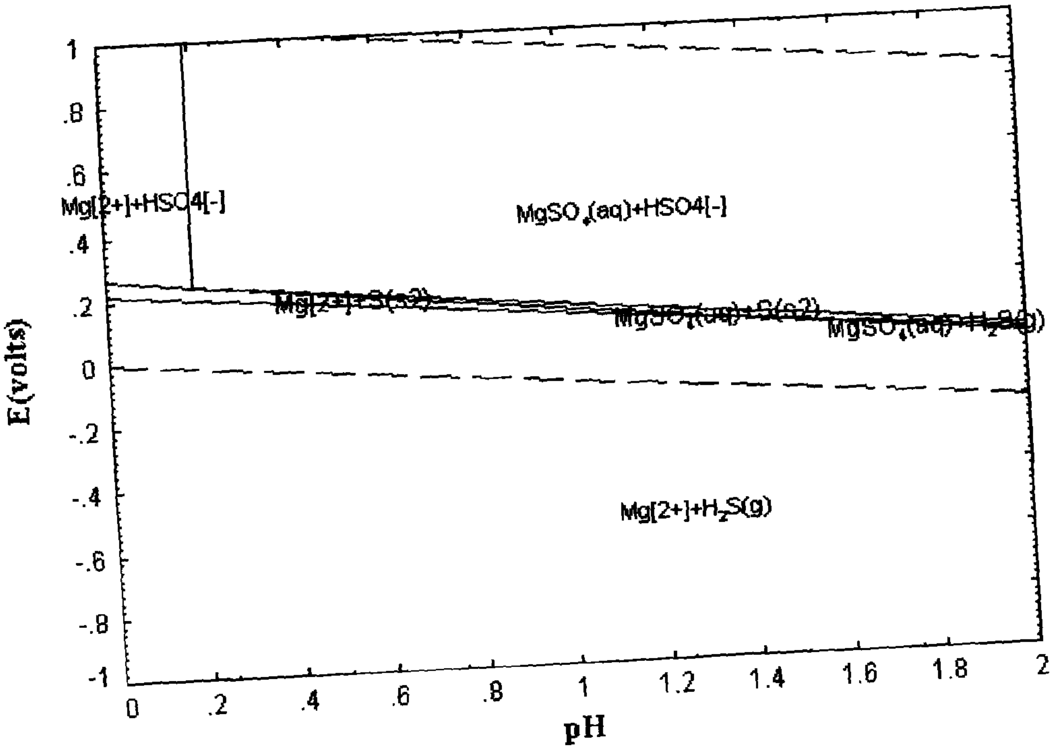
1
.8
.6
.4
.2
0
-.2
-.4
-.6
-.8
-1
E(volts)
0
.2
.4
.6
.8
1
1.2
1.4
1.6
1.8
2
pH
Mg[2+]+HSO4[-]
MgSO$_4$(aq)+HSO4[-]
Mg[2+]+S(s2)
MgSO$_4$(aq)+S(s2)
MgSO$_4$(aq)+H$_2$S(g)
Mg[2+]+H$_2$S(g)

Fig. 1.c.

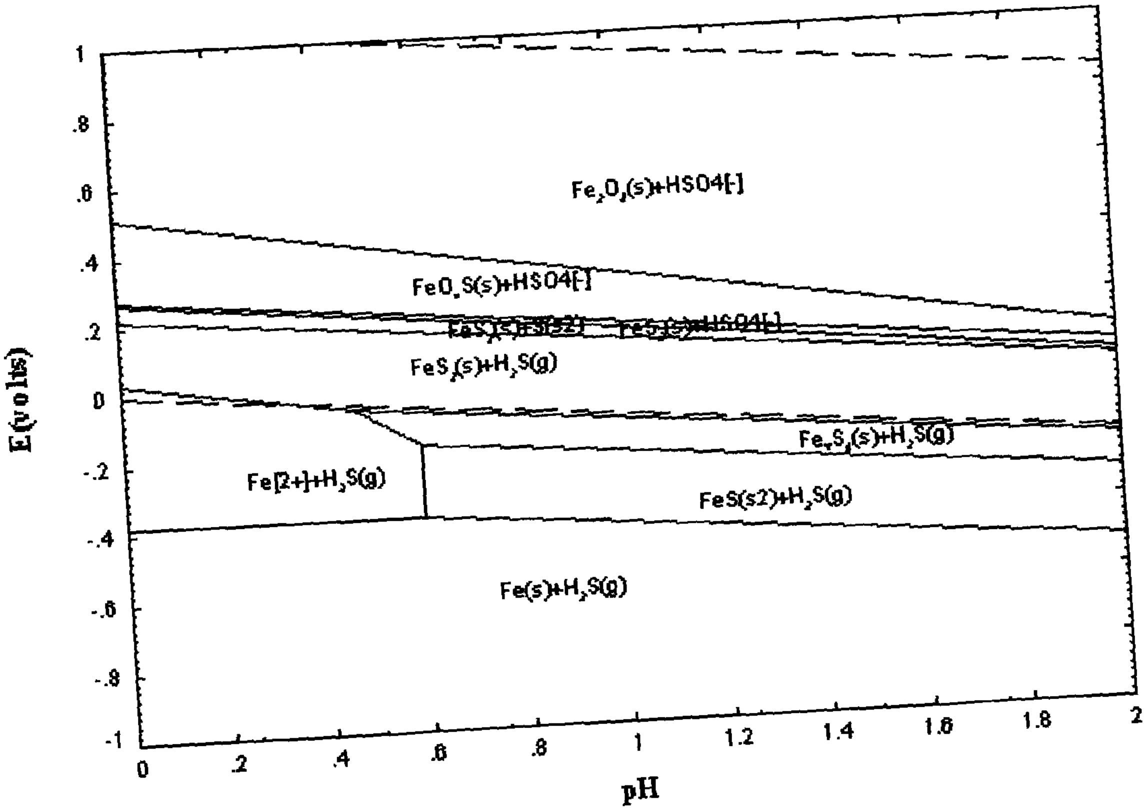
1
.8
.6
.4
.2
0
-.2
-.4
-.6
-.8
-1
E(volts)
0
.2
.4
.6
.8
1
1.2
1.4
1.6
1.8
2
pH
Fe$_2$O$_3$(s)+HSO4[-]
FeO$_4$S(s)+HSO4[-]
FeS$_2$(s)+S(s2)
FeS$_2$(s)+HSO4[-]
FeS$_2$(s)+H$_2$S(g)
Fe$_7$S$_8$(s)+H$_2$S(g)
Fe[2+]+H$_2$S(g)
FeS(s2)+H$_2$S(g)
Fe(s)+H$_2$S(g)

Fig.1.d.

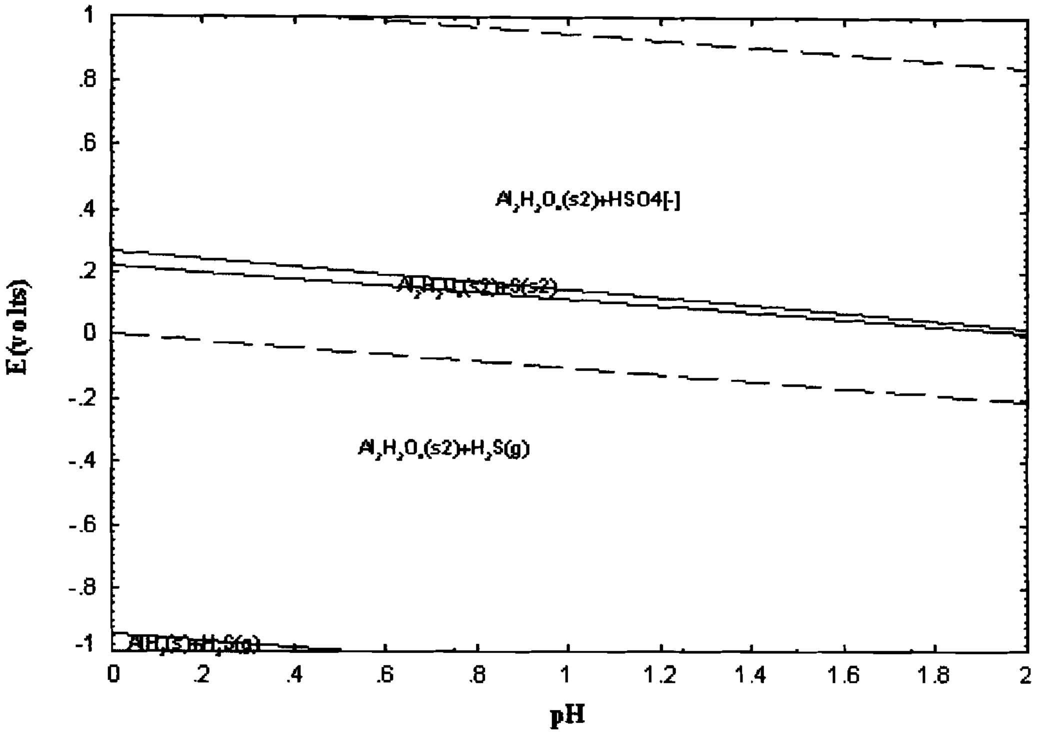
1
.8
.6
.4
.2
0
-.2
-.4
-.6
-.8
-1
E(volts)
$Al_2H_2O_4$(s2)+HSO4[-]
$Al_2H_2O_4$(s2)+S(s2)
$Al_2H_2O_4$(s2)+H_2S(g)
AlH_3(s)+H_2S(g)
0
.2
.4
.6
.8
1
1.2
1.4
1.6
1.8
2
pH

Fig.1.e.

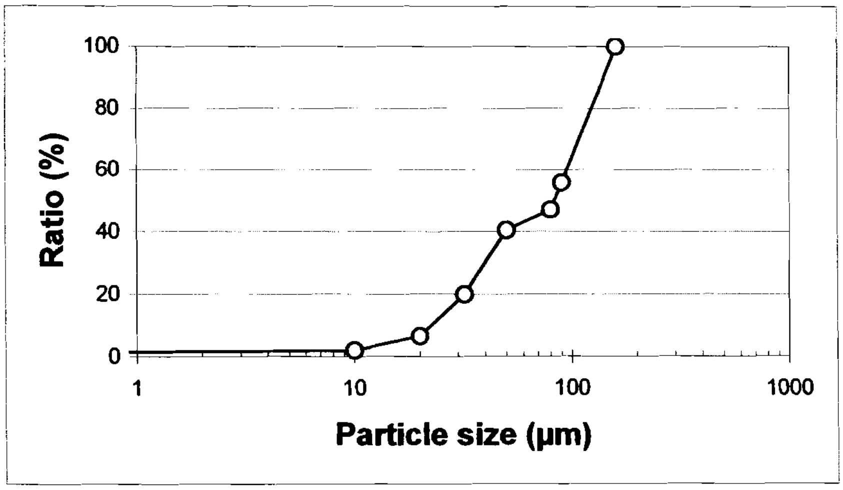
100
80
60
40
20
0
Ratio (%)
1
10
100
1000
Particle size (µm)

Fig. 2.

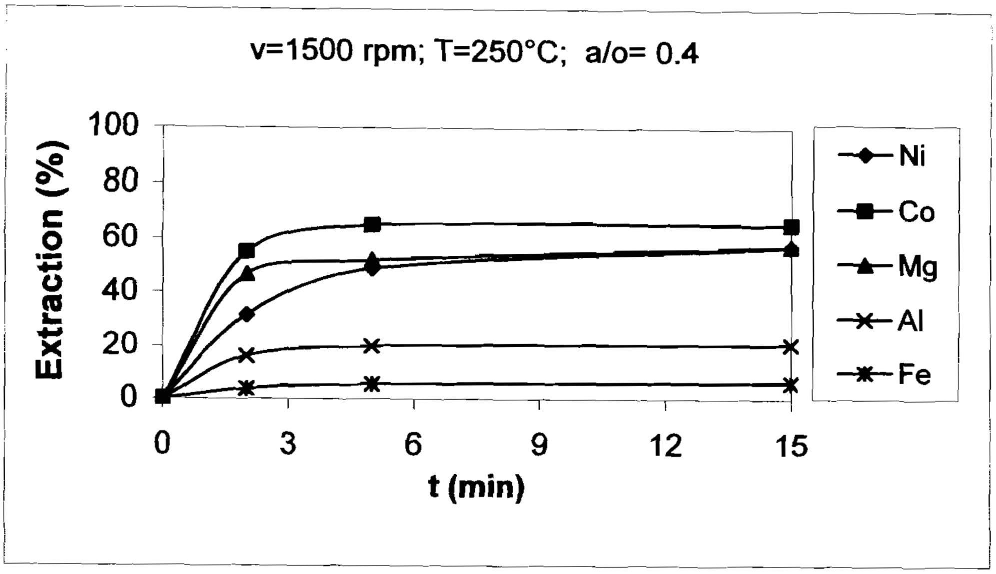
v=1500 rpm; T=250°C; a/o= 0.4
Extraction (%)
100
80
60
40
20
0
t (min)
0
3
6
9
12
15
Ni
Co
Mg
Al
Fe

Fig. 3.

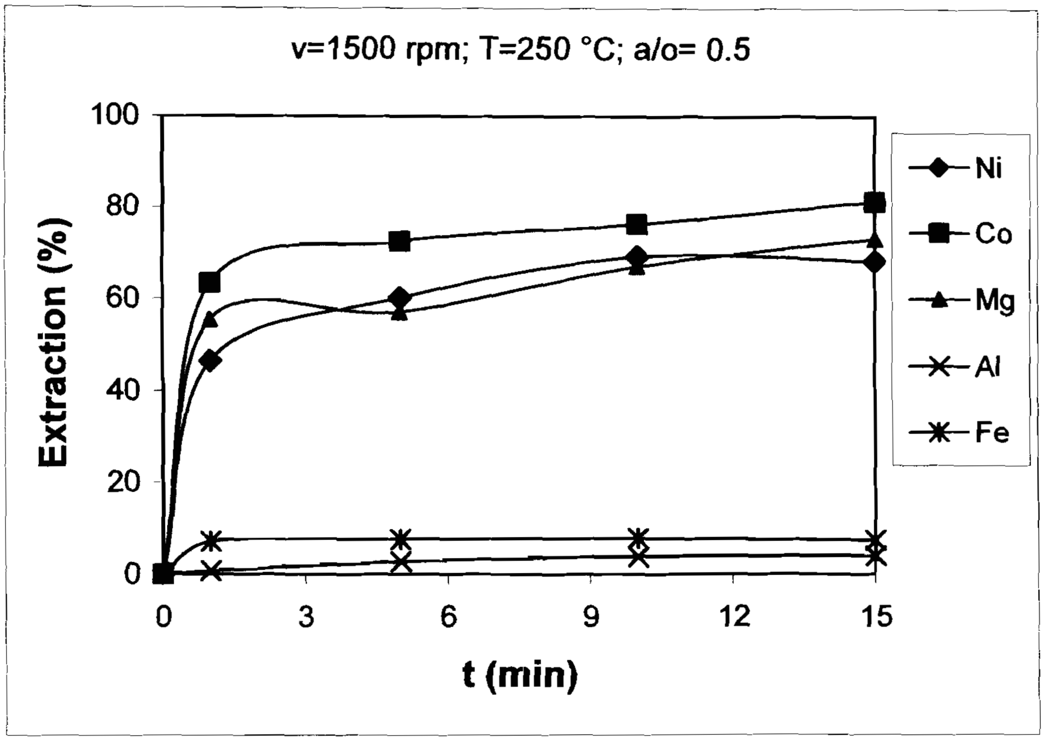
v=1500 rpm; T=250 °C; a/o= 0.5
Extraction (%)
100
80
60
40
20
0
t (min)
0
3
6
9
12
15
Ni
Co
Mg
Al
Fe

Fig. 4.

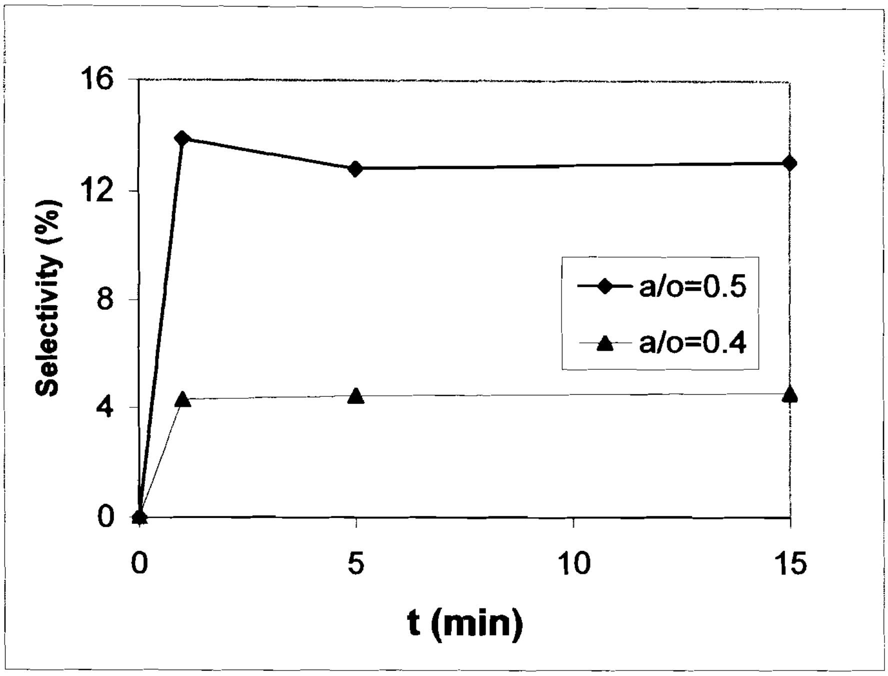
16
12
8
4
0
Selectivity (%)
0
5
10
15
t (min)
a/o=0.5
a/o=0.4

Fig. 5.

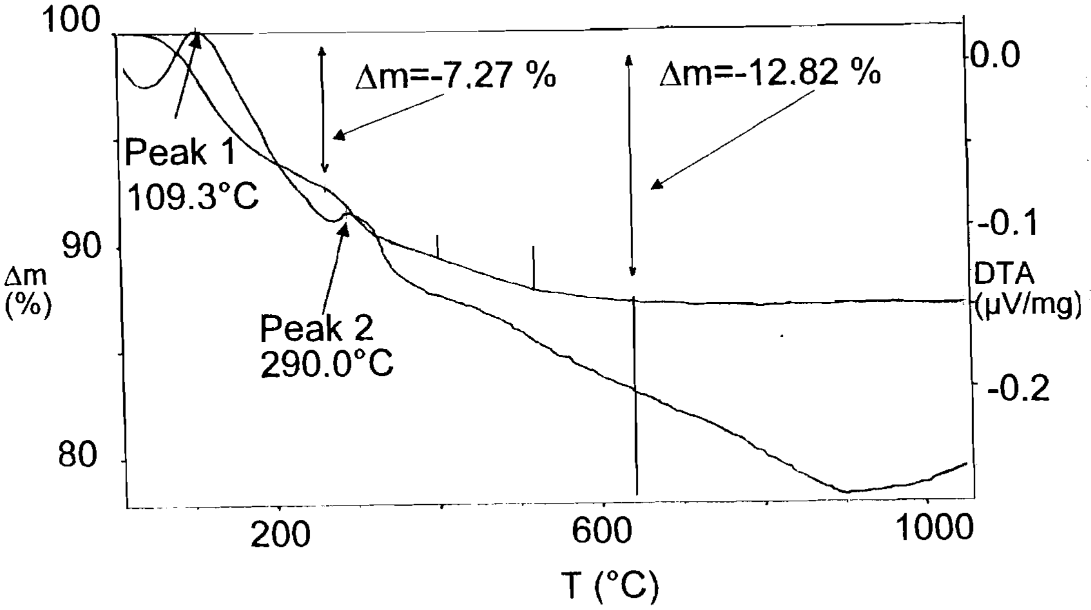
100
90
80
Δm (%)
0.0
-0.1
-0.2
DTA (μV/mg)
Δm=-7.27 %
Δm=-12.82 %
Peak 1
109.3°C
Peak 2
290.0°C
200
600
1000
T (°C)

Fig. 6.